# Virally delivered Channelrhodopsin-2 Safely and Effectively Restores Visual Function in Multiple Mouse Models of Blindness

M Mehdi Doroudchi[1], Kenneth P Greenberg[1,2], Jianwen Liu[3], Kimberly A Silka[4], Edward S Boyden[1,5], Jennifer A Lockridge[1], A Cyrus Arman[6], Ramesh Janani[1], Shannon E Boye[3], Sanford L Boye[3], Gabriel M Gordon[4], Benjamin C Matteo[1], Alapakkam P Sampath[6], William W Hauswirth[3] and Alan Horsager[1,4]

*[1]Eos Neuroscience, Inc., Los Angeles, California, USA; [2]Division of Neurobiology, University of California Berkeley, Berkeley, California, USA; [3]Department of Ophthalmology, University of Florida (UF), Gainesville, Florida, USA; [4]Institute for Genetic Medicine, University of Southern California (USC), Los Angeles, California, USA; [5]MIT Media Lab, Massachusetts Institute of Technology (MIT), Cambridge, Massachusetts, USA; [6]Zilkha Neurogenetic Institute, USC, Los Angeles, California, USA*

Previous work established retinal expression of channelrhodopsin-2 (ChR2), an algal cation channel gated by light, restored physiological and behavioral visual responses in otherwise blind *rd1* mice. However, a viable ChR2-based human therapy must meet several key criteria: (i) ChR2 expression must be targeted, robust, and long-term, (ii) ChR2 must provide long-term and continuous therapeutic efficacy, and (iii) both viral vector delivery and ChR2 expression must be safe. Here, we demonstrate the development of a clinically relevant therapy for late stage retinal degeneration using ChR2. We achieved specific and stable expression of ChR2 in ON bipolar cells using a recombinant adeno-associated viral vector (rAAV) packaged in a tyrosine-mutated capsid. Targeted expression led to ChR2-driven electrophysiological ON responses in postsynaptic retinal ganglion cells and significant improvement in visually guided behavior for multiple models of blindness up to 10 months postinjection. Light levels to elicit visually guided behavioral responses were within the physiological range of cone photoreceptors. Finally, chronic ChR2 expression was nontoxic, with transgene biodistribution limited to the eye. No measurable immune or inflammatory response was observed following intraocular vector administration. Together, these data indicate that virally delivered ChR2 can provide a viable and efficacious clinical therapy for photoreceptor disease-related blindness.

*Received 26 July 2010; accepted 14 March 2011; advance online publication 19 April 2011. doi:10.1038/mt.2011.69*

## INTRODUCTION

Retinitis pigmentosa and age-related macular degeneration cause severe vision loss or complete blindness in 15 million people worldwide,[1] a number that continues to increase with the aging population.[2] Recent gene therapy efforts have shown success in treating a relatively rare form of retinitis pigmentosa (*i.e.*, an RPE65 mutation) in human subjects.[3,4] However, the use of gene replacement therapy for vision loss is complicated by the genetic heterogeneity of retinal degeneration (nearly 200 different gene mutations are associated with retinitis pigmentosa),[5] retinal reorganization,[6] and photoreceptor death. Developing a broadly applicable gene therapy would restore vision in blind patients independent of the specific gene mutation and subsequent loss of photoreceptors by targeting a downstream point in the visual pathway.

Indeed, microelectronic retinal prostheses have shown fundamental success in generating visual percepts in blind subjects by stimulating spared neurons of the inner retina.[7–9] Still, activating these neurons require large disc electrodes (~20 times the diameter of a retinal ganglion cell body) leading to broad and indiscriminant activation of multiple cell types,[10,11] which will complicate the normal spatial and temporal processing of the retina.[12,13]

Several groups have demonstrated independently the building blocks for a successful therapy in which spared inner retinal neurons are sensitized to light using the algal light-gated cation channel, channelrhodopsin-2 (ChR2).[14,15] Bi *et al.* used a recombinant adeno-associated viral vector (rAAV) to express permanently and ubiquitously ChR2 in amacrine and ganglion cells of the *rd1* mouse. They demonstrated ChR2 expression restored photosensitivity at the retinal and cortical level.[16] Similarly, Lin *et al.* expressed melanopsin (Opn4), a mammalian light-sensitive protein, in non-melanopsin expressing ganglion cells, also demonstrating restored retinal photosensitivity and improvements in visually guided behavior.[17] However, direct optical stimulation of ganglion cells bypasses the inner retinal circuitry, where bipolar and amacrine cells shape the spatial and temporal properties of the visual input.[12,18] One exception is the recent work by

*M.M.D., K.P.G., and J.L. contributed equally to this work. A.P.S., W.W.H., and A.H. contributed equally to this work.*

***Correspondence:*** *Alan Horsager, Institute for Genetic Medicine, University of Southern California (USC), 2250 Alcazar Street, CSC 256, Los Angeles, California, 90089, 323–442-1978, USA. E-mail: horsager@usc.edu*

Greenberg *et al*., where ganglion cells were endowed directly with center-surround antagonism via differential targeting of opposing opsins.[19] Lagali *et al*. previously addressed this issue by delivering ChR2 to the ON bipolar cells of neonatal *rd1* mice using electroporation,[20] leading to physiological and behavioral responses to light stimuli.[21] Although groundbreaking, ChR2 was delivered to immature retinae using electroporation, a delivery method not suitable for clinical application as it leads to transient[22] and low expression levels (~7% of the targeted ON bipolar cells).

Here, we demonstrate the development of a clinically relevant therapy for late stage retinal degeneration using ChR2. Using a tyrosine-mutated rAAV to deliver the ChR2 transgene, we were able to establish targeted, robust, and long-term transgene expression in ON bipolar cells of the retina. Targeted ChR2 expression led to electrophysiological and behavioral improvements in visual function in three different mouse models of blindness (*rd1*, *rd10*, and *rd16*), with visual responses lasting at least 10 months postinjection (the longest time point measured). Finally, the safety profile of this therapy shows exclusive ocular localization of biodistribution, limited immune cell infiltration and inflammation, and an absent systemic immune response as measured through hematology, serum chemistry, and delayed-type hypersensitivity tests. Taken together, these data indicate that virally delivered ChR2 can provide a viable clinical therapy for photoreceptor disease-related blindness.

## RESULTS

### Transduction and targeted expression in retinal bipolar cells

To use ChR2 as a therapeutic agent to treat blindness, the transgene expression must be stable and robust in specific cellular targets. rAAV vectors with wild-type (WT) capsids have been shown to transduce effectively retinal ganglion cells following intravitreal injection,[16,17] and photoreceptors with subretinal injection.[23] However, the ability of WT rAAV capsids to penetrate significantly the inner retinal layers and transduce retinal bipolar cells remains unknown. Our tests of multiple WT rAAVs reveal very limited expression of humanized and enhanced green fluorescent protein (heGFP) in the inner nuclear layer when using a cell-specific promoter (data not shown). The limited efficacy of bipolar cell transduction using rAAVs with WT capsids is believed to involve the ubiquitin proteasome pathway during intracellular trafficking of rAAV particles, beginning with phosphorylation of tyrosine residues on the capsid surface.[24] Recently, engineered viral proteins that replace the tyrosine capsid residues with phenylalanine have resulted in 20-fold improvement in cellular transduction.[25] We sought to determine whether these vectors could transduce effectively diseased tissue and found a tyrosine capsid-mutated serotype that was particularly effective at transducing bipolar cells of the diseased retina in *rd1*, *rd10*, and *rd16* mice—an rAAV8 (with a single point mutation at the Y733F tyrosine to phenylalanine), AAV8-Y733F.

We injected subretinally the AAV8-Y733F virus packaged with an *mGRM6-SV40-hChR2-heGFP* vector in the *rd10* mouse (**Figure 1a**; see Materials and Methods section) at ~8 weeks of age and evaluated the expression of the hChR2–heGFP fusion protein 10 weeks later (*i.e*., 4.5 months of age) by immunolabeling for heGFP and PKCα, a rod bipolar cell marker. Using the *mGRM6* enhancer, we targeted expression of our transgene in ON bipolar cells, including both rod bipolar and ON cone bipolar cells (**Figure 1b,e,f**).[20] Although we found no residual photoreceptors in these *rd10* mice when tissue was stained with an antibody against rod arrestin (**Figure 1b**), the integrity of the inner nuclear layer and the dendritic processes that connect with ganglion cells was well maintained (**Figure 1c,d**), consistent with previous studies.[26] We observed transgene expression in

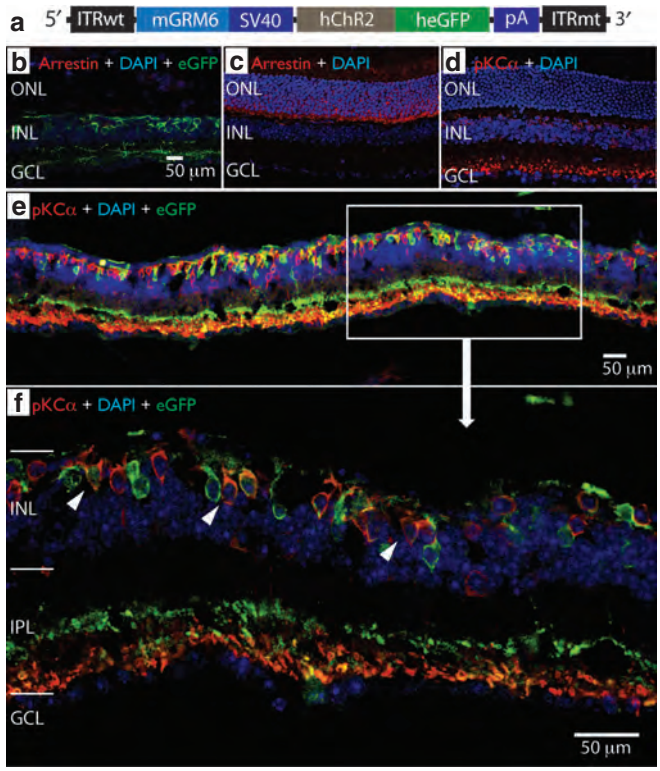


**Figure 1 hChR2-heGFP is selectively targeted and expressed in ON bipolar cells in *rd10* mice.** (**a**) The self-complementary vector construct contained one wild-type AAV2 terminal resolution site (ITRwt) and one mutant resolution site (TR) (ITRmt), which was packaged in a capsid tyrosine-mutated recombinant adeno-associated viral vector (rAAV8)-Y733F. The regulatory region consisted of a 200 bp enhancer region from the murine *GRM6* gene fused to a 203 bp SV40 core promoter. The transgene consisted of a mammalian optimized channelrhodopsin-2 (hChR2, 930 bp) fused to a humanized and enhanced green fluorescent protein (heGFP, 700 bp). A polyadenylation signal sequence (β-globin pA, 210 bp) was included. (**b**–**f**) Confocal images of the retina showing targeted eGFP expression in the ON bipolar cells of an *rd10* mouse retina. (**b**) The absence of arrestin suggests a complete loss of photoreceptors. (**c**,**d**) Arrestin and PKCα stain of normal retina, showing normal photoreceptor layers and rod bipolar cells. (**e**,**f**) eGFP expression in *rd10* retina following subretinal delivery of AAV8-Y733F vector. hChR2 fused with heGFP is indicated in green in the above confocal images. Red is PKCα, a marker for rod bipolar cells, a type of ON bipolar cell in the inner nuclear layer (INL). Blue is DAPI which stains for cell nuclei. Yellow indicates colocalization of hChR2-heGFP and PKCα expression, thus showing expression of the transgene in rod bipolar cells. We find transgene expression in both rod bipolar cells (yellow) and ON cone bipolar cells (green only), suggesting that we have targeted transgene expression of the entire ON bipolar cell population, which includes both rod and ON cone bipolar cells. Note the robust expression in the inner portion of the inner plexiform layer (IPL) as well, further indication of hChR2-heGFP expression in both ON cone and rod bipolar cells. (**e**) ×20 magnification confocal image. (**f**) ×63 magnification confocal image of the indicated area. White arrows indicate heGFP expression in the target cells (*i.e*., ON bipolar cells).

the soma as well as the finely branched dendrites of ON bipolar cells, indicating robust expression was achieved (**Figure 1e,f**). As a further confirmation of the specificity of the *mGRM6* enhancer sequence to ON bipolar cells, we observed a clear delineation of the strata in the inner plexiform layer, showing colocalization of heGFP and PKCα in rod bipolar cells at the proximal limits of the inner plexiform layer, and strong expression of heGFP in the ON sublamina of the inner plexiform layer (**Figure 1f**).

Unlike previous efforts,[21] ChR2 expression in these experiments was long-lasting. We evaluated the expression of the transgene delivered with the AAV8-Y733F vector at 10 weeks and 10 months postinjection (**Figure 2**). We found that expression was stronger at 10 weeks but significant expression in ON bipolar cells was observed through 10 months (the latest time point evaluated). Furthermore, this long-lasting expression translated into maintained behavioral efficacy at this same 10-month time point (see below). Thus, robust, targeted expression in ON bipolar cells of degenerated retina was achieved using a rAAV capsid tyrosine-mutated viral vector.

## Physiological efficacy

In the normal human visual system, the retina is responsive to light levels between $10^4$ and $10^{16}$ photons/cm$^{-2}$/s,[27] whereas it was found that physiological spiking in ChR2-expressing retinal ganglion cells in mice required at least ~$1.2 \times 10^{14}$ photons/cm$^{-2}$/s.[18] Determining threshold sensitivity is valuable as it serves to inform the luminance conditions under which this therapeutic approach could provide useful vision. In mouse models of retinal degeneration, measures of threshold sensitivity for action potential generation in retinal ganglion cells reveal whether bipolar-derived ChR2 responses are sufficiently robust to activate higher visual centers. Furthermore, measuring threshold sensitivity serves to answer whether the synaptic connectivity remains functionally intact in the inner plexiform layer in the context of a degenerated and potentially remodeled retina.[6]

We assessed the light-driven activity of ganglion cells in 24-week old *rd10* mice that received a subretinal injection of the AAV8-Y733F vector 16 weeks earlier. We determined the minimum light level necessary to activate ChR2-expressing ON bipolar cells (*i.e.* threshold), and how the rate of action potential generation changed as a function of increasing light intensity using a multielectrode array during full-field illumination (450–490 nm blue light) (**Figure 3**). In total, we observed light-evoked responses during illumination in six ganglion cells across three injected retinas. At the lower light limit, we observed reliable light-evoked ganglion cell firing in response to steps (**Figure 3a**) with an intensity of $4 \times 10^{16}$ photons/cm$^{-2}$/s, within the range of light intensities encountered in bright daylight. Ganglion cell responses persisted during perfusion of an mGluR6 agonist (APB) that blocks photoreceptor to ON bipolar cell communication, confirming the signal originated in ChR2-expressing ON bipolar cells rather than residual photoreceptors. Responses were completely eliminated during perfusion of antagonists for NMDA and ionotropic glutamate receptors (CPP and CNQX), confirming that light responses originated presynaptically rather than from intrinsically photosensitive retinal ganglion cells (**Figure 3a,b**). Multielectrode array experiments from 24-week-old uninjected control retinas showed no light-evoked activity, consistent with photoreceptor loss in these degenerated *rd10* mice. Finally, the action potential frequency increased with increasing light intensity (**Figure 3c**). Taken together, these results suggest that AAV-mediated expression of ChR2 in ON bipolar cells can drive robust light-evoked responses in diseased retinas at luminance levels normally encountered during daylight activity.

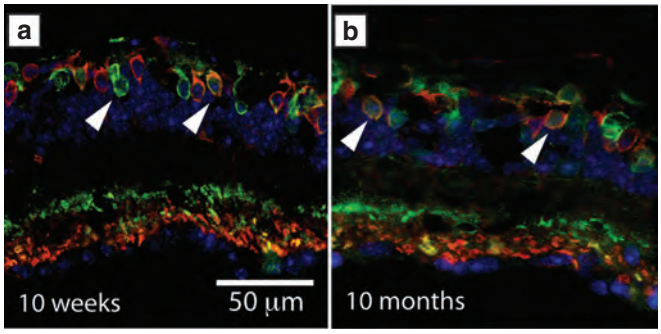


**Figure 2 hChR2-heGFP is maintained over time.** We evaluated expression of our transgene at multiple time points postinjection, (**a**) 10 weeks and (**b**) 10 months. Expression appeared to slightly decrease over time but there was still significant transgene expression even at the 10-month time point. White arrows indicate humanized and enhanced green fluorescent protein (heGFP) expression in the target cells (*i.e.*, ON bipolar cells). hChR2, human codon-optimized channelrhodopsin-2.

## Behavioral efficacy

Quantifying visual function in mice has been approached using several behavioral paradigms including light avoidance tasks[28] and measurements of the optokinetic response with rotating gratings.[29] Although these tasks provide information about light sensitivity and responsiveness to spatially organized stimuli, the quality of the mouse's visual experience remains unclear because these responses do not necessarily involve cortical circuits. Alternatively, a visually guided behavioral task involving choice-decisions ensures that visual information is processed cortically and perceptual experience has occurred.

We evaluated visual function in two different mouse models of blindness (*i.e.*, *rd1* and *rd16*) using a visually guided behavioral task, where the test groups consisted of *rd1* mice injected with saline solution (sham controls), *rd1* and *rd16* mice injected with rAAV8-Y733F packaged with the *mGRM6-SV40-hChR2-heGFP* vector, and uninjected WT C57Bl/6 mice (*i.e.*, normally sighted). The behavioral task required mice to find an escape platform within a water maze apparatus (**Figure 4a**) that was associated with a light stimulus (**Figure 4b**), and the time to find the escape platform was measured.[30,31] During the training period the photon flux of the white light stimulus at 470 nm, as measured from the center of the maze (*i.e.*, where the each mouse begins their trial), was ~$3.5 \times 10^{18}$ photons/cm$^{-2}$/s. For the sham-injected mice and the treated mice, 14 training sessions were conducted; for the WT, 7 training sessions were conducted. In both instances, the training was sufficient for the average time to find the target to reach an asymptote. After 14 days of training, the ChR2-treated mice were able to reach the escape target 2.5-fold faster than the sham-injected controls, with ChR2-treated mice escaping the maze at 7.0 ± 2.9 seconds (mean ± SEM), whereas their untreated counterparts took 19 ± 6.0 seconds on the last day of training. For comparison, WT mice took 2.6 ± 0.7

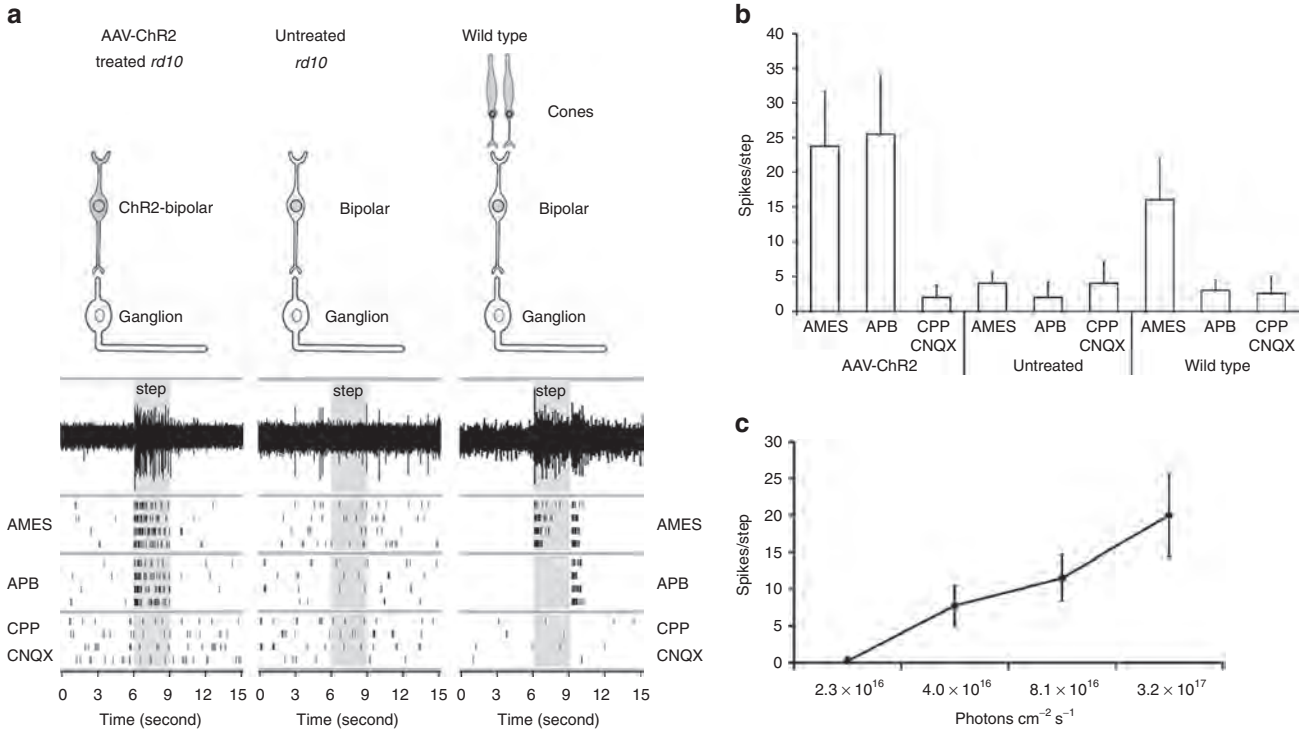


**Figure 3 Adeno-associated viral vector (AAV)-mediated delivery of channelrhodopsin-2 (ChR2) targeted to ON bipolar cells restores photosensitivity to blind *rd10* mouse retinae.** (**a**) Examples of ChR2-mediated responses originating in bipolar cells to 3- second light steps recorded in postsynaptic ganglion cells. Sustained action potential generation was observed during perfusion with Ames media and during perfusion with Ames media containing the metabotropic glutamate receptor 6 (mGluR6) receptor agonist (APB) demonstrate that light responses originate from bipolar cells rather than photoreceptors. Perfusion of glutamate receptor antagonists (CPP/CNQX) abolishes light-evoked activity, suggesting that light responses are presynaptic to ganglion cells and are not mediated by intrinsically photosensitive retinal ganglion cells (ipRGCs). Untreated *rd10* retinae show no light-evoked activity under control or pharmacological block conditions. An increase of spontaneous activity in degenerated *rd10* retinae is observed when compared to wild type. Control wild type (C57BL/6) retinae exhibit transient ON/OFF responses to full-field illumination under control conditions. ON component of the response is blocked in APB, and light response is eliminated entirely under glutamate block. (**b**) Spike number in response to flashes for AAV-ChR2 treated ($n = 6$), untreated ($n = 8$), and wild-type ($n = 10$) retinae under control, APB, and CPP/CNQX conditions. Responses of treated *rd10* retinae are significantly different ($P = 0.01$) than baseline firing of untreated *rd10* controls. Error bars represent SE of the mean. (**c**) Spike activity of AAV-ChR2-treated retinae in response to flashes of increased intensity.

**Table 1 Detection of rAAV vector sequences by quantitative PCR in *rd10* mice**

| | 1 Week postinjection | | | | | | 10 Weeks postinjection | | | | | |
|---|---|---|---|---|---|---|---|---|---|---|---|---|
| | C1 | C2 | T1 | T2 | T3 | T4 | C1 | C2 | T1 | T2 | T3 | T4 |
| Eye | — | — | 1.21 | 0.71 | 0.63 | 1.32 | — | — | 2.45 | 2.33 | 0.29 | 1.49 |
| Heart | — | — | — | — | — | — | — | — | — | 0.07 | — | — |
| Lung | — | — | — | — | — | — | — | — | — | — | — | — |
| Liver | — | — | — | — | — | 0.18 | — | — | — | — | — | — |
| Kidney | — | — | — | — | — | — | — | — | — | — | — | — |
| Jejunum | — | — | — | — | — | — | — | — | — | — | — | — |
| Skin | — | — | — | — | — | — | — | — | — | 0.15 | — | — |
| Spleen | — | — | — | — | — | — | — | — | — | 0.09 | — | — |
| Brain | — | — | — | — | — | — | — | — | — | — | — | — |
| Gonad | — | — | — | — | — | — | — | — | — | — | — | — |
| Lymph | — | NA | — | NA | — | — | — | — | — | — | — | — |
| Muscle | — | — | — | — | — | — | — | — | — | 0.17 | — | — |

*Abbreviations*: ChR2, channelrhodopsin-2; rAAV, recombinant adeno-associated viral vector.
Control mice are labeled with "C" and AAV8-Y733F-treated mice with "T". Values are the number of ChR2 copies per β-actin copy of DNA for each tissue. A threshold value of 0.05 was applied and values below this threshold were not reported.

seconds on their last day of training. The training data is shown in **Supplementary Figure S1**.

After the mice were fully trained on the task, we evaluated their performance at different illumination levels to determine the minimum light necessary to improve behavioral performance (*i.e.*, perceptual threshold). Behavioral performance was measured in increments of tenfold in light intensity between $3.5 \times 10^{12}$ and $3.5 \times 10^{18}$ photons/cm$^{-2}$/s (**Figure 4c,d**). At lower light intensities, we did not observe a significant difference in behavioral performance between the ChR2-treated mice and the sham-injected controls. However, we observed a significant improvement in the performance of the ChR2-treatment group (*i.e.*, decreased time to find the escape platform) as the intensity of the target increased (**Figure 4c,d**). Sham-injected controls were able to develop strategies to escape the maze that reduced their time to escape. However, these escape times never approached those of the WT or ChR2-treated mice. The performance of the WT and the ChR2-treated mice overall the light levels were nearly threefold improved relative to the sham injected control group ($P < 0.0001$, as measured with a Kruskal–Wallis analysis of variance). The performance of all treated *rd* mice were significantly better than their untreated counterparts, establishing this therapy could be applied to multiple genetic forms of retinitis pigmentosa. Finally, we evaluated a subset of six animals treated with the AAV8-Y733F vector at ~10 months postinjection and found that these mice maintained their ability to perform the task as well as earlier time points, and performed significantly better than their untreated counterparts ($P < 0.0001$).

## Exploratory safety studies

We completed a safety study of our vector, AAV8-Y733F (*mGRM6-SV40-hChR2-heGFP*), as the first step in a broader preclinical development program. Following to US Food and Drug Administration guidelines, we identified biodistribution, ocular toxicology including phototoxicity, and systemic immunity as the key necessary preliminary data for developing a safety profile of the therapeutic agent. **Supplementary Table S1** provides an overview of all treatment groups in the safety studies.

***Biodistribution.*** We evaluated both the distribution of the hChR2 DNA [through quantitative PCR (qPCR)] and expression (using immunohistochemistry and confocal imaging) in 12 different tissues, including the injected eye, at two different time points (1 week and 10 weeks postinjection). qPCR analysis showed the presence of hChR2 DNA in all treated eyes but in none of the uninjected control eyes (**Table 1**). Small quantities of hChR2 DNA were found in four tissues outside of the treated eyes, but the tissues were all of different types, suggesting that the presence of hChR2 DNA was due to either cross-contamination or nonspecific binding of our probe tag (SYBR green). Biodistribution was further evaluated by measuring hChR2-heGFP transgene expression. We find that 1 and 10 weeks after injection, the AAV8-Y733F injected eyes were positive but the control balanced salt solution (BSS) injected eyes were negative for heGFP staining. No heGFP immunoreactivity was detected in other distant organs of control and AAV-injected mice (**Supplementary Figure S2**).

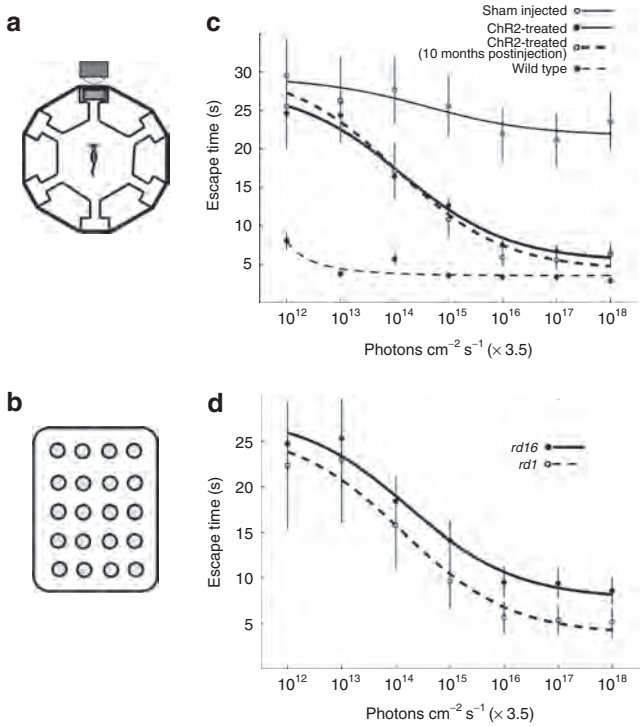


**Figure 4 Expression of hChR2-heGFP leads to improved visual performance.** (**a**) The schematic for the water maze used to measure perceptual threshold (*i.e.*, the minimum light necessary to guide the escape behavior). The escape platform was tethered to a full spectrum 5 × 4 LED array target (**b**) with a maximum blue light output of $3.5 \times 10^{18}$ photons/cm$^{-2}$/s as measured at 470 nm. The ambient light of the room was dim and at least two orders of magnitude below the LED array target output. After 14 training sessions, escape time was measured at different light levels (x axis in **c** and **d**). We compared the behavioral performance of *rd1* and *rd16* mice treated with AAV8-Y733F (*mGRM6-SV40-hChR2-heGFP*) (**c**) relative to the performance of untreated *rd1* mice and normally sighted wild-type C57Bl/6 mice. Generally, both the *rd1* and *rd16* mouse models of blindness had improved escape times as a function of increasing light intensity, however, *rd1* mice appear to perform better than *rd16* (**d**). hChR2, human codon-optimized channelrhodopsin-2; heGFP, enhanced green fluorescent protein.

***Ocular toxicity.*** An ocular toxicity study was conducted to evaluate anatomical changes (*i.e.*, changes in cell layer thickness), immune cell infiltration, inflammatory response, and phototoxicity (*i.e.*, impact of chronic high-intensity light exposure) using a high and low vector dose (**Figure 5**). In conjunction with our earlier work in primate cortex,[32] no morphological changes in retinae were observed via hematoxylin and eosin staining or immunohistochemistry. No CD45 expression was found at either the high or low dose level, suggesting limited or no presence of immune cells in the retina or vitreous. Glial fibrillary acidic protein (GFAP) was noted on the vitreal side of the retina in both treatment and control conditions, consistent with increases observed following photoreceptor degeneration.[33] Furthermore, we observed significant GFAP expression in noninjected control animals.

Although we have established that our therapy can be used within the response range of normal human vision, it may be necessary to present stimuli at higher intensity levels (via an optical delivery device) to utilize the full dynamic range and chromatic spectrum of the environmental light levels. To determine

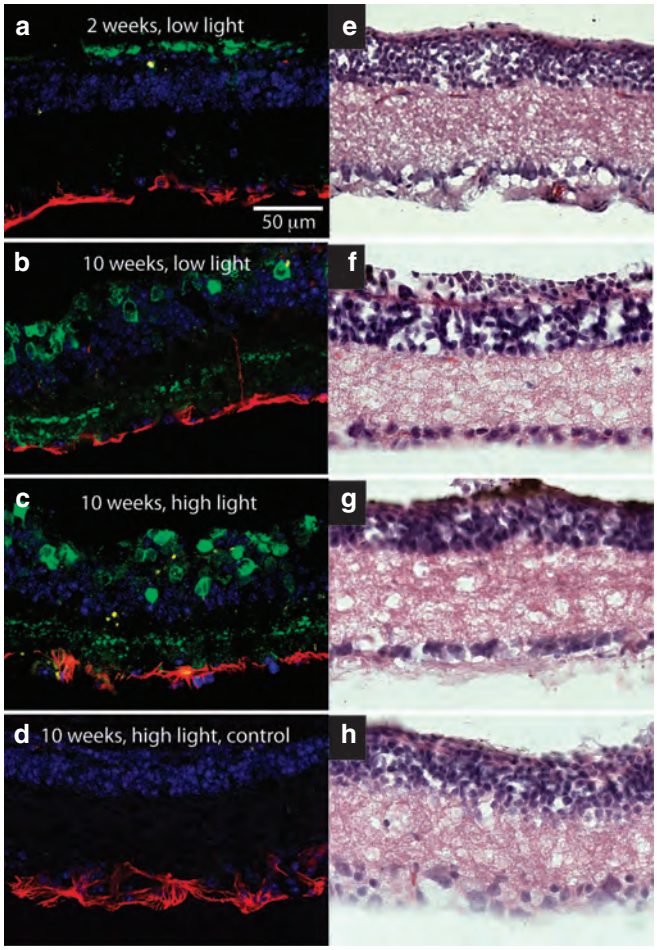


Figure 5 Toxicological evaluation of the retina. Evaluation of ocular toxicology using confocal microscopy and four-color immunostaining. DAPI (blue), heGFP (green), CD45 (yellow), a general marker for immune cells, and GFAP (red), a marker for astrocytes, were used to label the retinae in the different conditions. Hematoxylin and eosin (H&E) staining (column 2) was used to evaluate overall retinal structure. We evaluated tissue at two different time points, 2 and 10 weeks, and at two different light intensities (low and high). See Materials and Methods section for more details on experimental parameters.

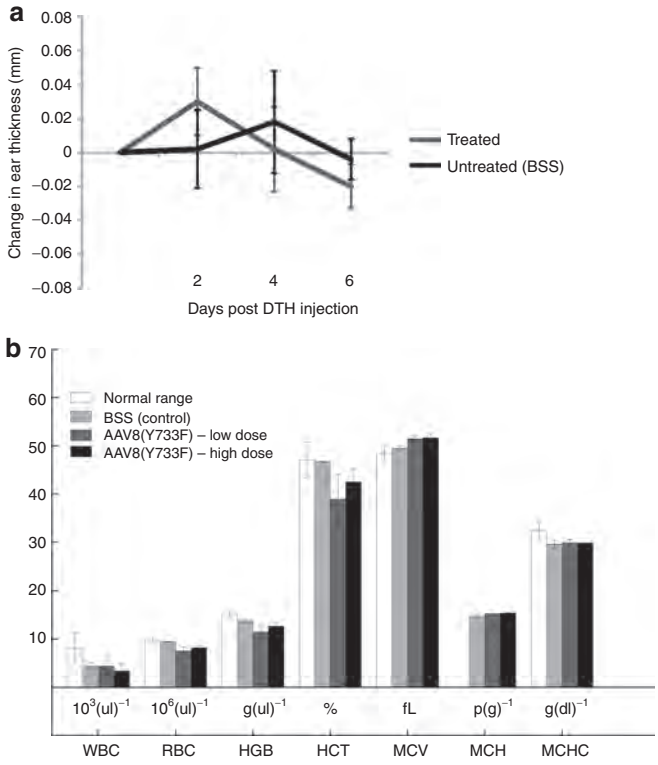


Figure 6 Systemic evaluation of immunogenicity. (**a**) Subcutaneous injection of AAV8-Y733F(mGRM6-SV40-hChR2-heGFP) in the right ear of rd10 mice to determine the extent of delayed-type hypersensitivity (DTH) response. No significant differences were observed at any time postinjection. Error bars indicate SE of the mean. (**b**) complete blood count (CBC).

the potential phototoxic effects of chronic high-intensity light stimulation we exposed control or ChR2-treated mice to high-intensity light ($3.5 \times 10^{18}$ photons/cm$^{-2}$/s) for 10 weeks, and did not observe significant changes in retinal structure, CD45 expression, or GFAP expression (**Figure 5**).

***Systemic immunity.*** Although the viral vector was not detected outside the injected eye and no toxicity was documented, we still determined the systemic response to the introduction of the therapy. The delayed-type hypersensitivity skin test is used to determine whether prior exposure to an antigen has occurred. If the formation of T cells, including both CD4$^+$ and CD8$^+$, has occurred as a function of the introduction of the therapy, injection of a small amount of the test article under the skin will result in induration, swelling, and monocytic infiltration within 1–3 days.[34,35] Five days after subretinal delivery of AAV8-Y733F (*mGRM6-SV40-hChR2-heGFP*), mice were injected with a second dose of vector subcutaneously in the right ear at the same dosage and volume. Delayed-type hypersensitivity reactions were monitored 1, 2, 4, and 6 days postinjection by evaluation of inflammatory changes and measuring ear thickness. No sign of inflammation (swelling or redness) was observed in the ear of the injected mice, and no difference in thickness was measured (**Figure 6a**). In addition, immunohistochemical analysis of tissue sections of the ears from the animals injected with the test article did not show any CD45 immunoreactivity indicating the absence of infiltrated immune cells or local inflammation within the ear following injection.

Additionally, we evaluated the hematological profile of ChR2-treated animals via comprehensive complete blood count and comprehensive serum chemistry analysis. The complete blood count values measured (**Figure 6b**) included the following: white blood cell count, red blood cell count (RBC), hemoglobin concentration, hematocrit, mean corpuscular volume, amount of hemoglobin per RBC (MCH), and the concentration of hemoglobin per RBC (MCHC). Each of these was within the normal range, indicating that there was no hematologically measurable immune response. **Supplementary Table S2** shows the serum chemistry analysis of *rd10* mice 10 weeks postinjection in control BSS, low-dose, and high-dose injected animals.

## DISCUSSION

We describe a broadly applicable translational therapy for restoring visual function in patients suffering from photoreceptor degeneration, regardless of the underlying genetic cause. We

targeted transgene expression to the ON bipolar cells using the *mGRM6-SV40-hChR2-heGFP* construct packaged in a tyrosine capsid-mutant AAV vector. This therapy produces stable expression lasting at least 10 months (the longest time point measured) after a single injection, with electrophysiological and behavioral efficacy maintained during this period. Additionally, the efficacy of this therapy is independent of the nature of the retinal degeneration tested (*i.e.*, providing behavioral and physiological improvements in multiple mouse models of retinal degeneration), suggesting broad applicability to the diverse genetic causes underlying photoreceptor degeneration. Finally, a toxicological and safety evaluation provides initial evidence that supports a safe therapy.

## Transgene expression is targeted and stable in diseased retina

Developing synthetic promoters to target transgene expression to a specific subtype of cell is at least arduous. In addition, changes in the expression profile as a function of disease further complicate this process. In mouse models of retinal degeneration there is significant evidence of reorganization[6] (but see ref. 26). In addition, there are changes in gene expression including a substantial decrease in metabotropic glutamate receptor 6 (mGluR6) in the ON bipolar cells after dendritic tree retraction.[36] This brought into question whether or not we could use a synthetic promoter sequence previously designed to target ON bipolar cells of the normal retina.

Here, we were able to targeted expression of ChR2 to the ON bipolar cells using a 200 bp mGRM6 regulatory sequence that contained essential transcription factor binding sites for the transcription factors (TFs) Pax6 and Pou3f2 in multiple mouse models of blindness. Mutating any one of these sequences has been found to lead to a significant decrease in transgene expression.[20] However, it was found that expression of these TFs were upregulated over time in the *rd1* mouse.[37] Indeed, we were able to obtain significant expression in *rd* retinae, suggesting that these TFs are still readily expressed.

Surprisingly, we found an apparent increase in the overall expression levels of our transgene when chronically exposed to high-intensity light. This suggests that chronic activation of ChR2 may very well lead to a change in gene regulation, ultimately increasing the amount of protein being synthesized.[38] This effect could be the result of an increased cellular activity, thus upregulating transcriptional activity.[39] This suggests that the expression of Pax6 and Pou3f2 may be activity dependent and increase over long-term light exposure in ChR2-treated tissue.

## Behavioral and physiological efficacy is due to direct bipolar cell activation

Visual perception in retinally degenerated animals may be mediated by either intrinsically photosensitive retinal ganglion cells or residual photoreceptors. It is well known that photosensitive melanopsin ganglion cells contribute to pupillary light reflexes and circadian rhythm.[40,41] However, it remains unclear how these cells may contribute to image formation, as the temporal responsiveness of these proteins is sluggish,[41,42] and their projections are not entirely known. In our untreated *rd* animals, we did find a slight behavioral improvement as a function of increasing light level (**Figure 3c**) and clear improvement on the task during training (**Supplementary Figure S1b**). However, behavioral improvements between treated and untreated animals in our studies were substantial and suggest that, even if there are contributions to visual image formation by melanopsin-expressing ganglion cells, these contributions are minimal.

Recent findings have shown that transgenic *rd1* mice expressing ChR2 in retinal ganglion cells under the *thy1* promoter do not have improved visual behavior. Additionally, it was suggested that any improvements in behavioral efficacy of both ChR2 transgenic *rd1* mice and untreated *rd1* mice was due to small patches of residual cone photoreceptors.[18] Although this does bring into question the ability of ChR2 to rescue vision, we believe this is not inconsistent with our findings for the following reasons: (i) we are targeting ON bipolar cells rather than both ON and OFF ganglion cells (as is the case when using the *thy1* promoter), thus utilizing physiological circuitry that allows for the proper processing of visual information.[13,21] Targeting and driving ON and OFF cells, simultaneously, could distort the normal physiological signaling of the retina. (ii) This behavioral task was significantly more difficult than the task used by Thyagarajan *et al*. (a 6-alternative forced choice rather than a 2-alternative forced choice), which may magnify the differences in visual behavior performance between ChR2-treated and untreated mice. (iii) The contrast between the target stimulus and nontargets in our tests were about 2 log units less than those used by Thyagarajan *et al*. This decreased contrast would make the task more difficult. (iv) Finally, through selective pharmacological block of synaptic transmission, we demonstrate that light responses in treated retinae originate from ON bipolar cells, and not from intrinsically photosensitive retinal ganglion cells or residual photoreceptors.

By targeting the bipolar cells rather than ganglion cells, we are able to take advantage of neural convergence from bipolar to ganglion cells, increasing signal amplification and the potential for photon catch.[43] Additionally, the use of tyrosine-mutated capsid AAVs appears to increase our transduction efficiency, leading to an increase in overall transgene expression in our target cells. We found that we could improve visual performance in ChR2-treated mice with full chromatic white light levels as low as $3.5 \times 10^{14}$ photons/cm$^{-2}$/s, similar to physiological recordings in previous studies.[18] Light sensitivity of this level could enable functional outdoor vision without the aid of light amplifying hardware, though such a device may be required indoors. Taken together, our physiological and behavioral data suggest that the virally delivered introduction of hChR2 into the ON bipolar cells of the mouse retina improves visual function as measured with a visually guided detection task. The tyrosine-mutant vectors are more effective at improving this visual behavior and benefits are maintained many months past the introduction of the therapy.

## Virally delivered ChR2 shown to be safe in our preliminary non-GLP safety evaluation

This was the first comprehensive safety study that combines the use of light-sensitive proteins with a tyrosine-mutated capsid AAV to restore functional vision. Although neural interrogation using opsins has been studied in more than a hundred papers with an eye toward future clinical application, very little data has been

generated to evaluate the safety profile of these proteins. Here, we establish an in-depth safety profile. We find these proteins are not toxic, do not generate an immune response, and remain functional for months, consistent with previous data showing stable cell membrane properties and an absence of immune response in the macaque brain.[32] Also, animals exposed to our therapy do not generate a cell-mediated immunity (*i.e.*, T-cell generation).

A concern of using ChR2 as a tool to rescue vision is the requirement of high-intensity light to activate the molecule.[15] Indeed, there is evidence that chronic exposure to high intensity light can induce apoptosis in retinal cells, specifically photoreceptors.[44] However, it remains unclear whether apoptosis occurs in other retinal cells such as bipolar or ganglion cells under these environmental conditions. We chronically exposed our *rd10* ChR2-treated mice to either 1 week or 10 weeks of high intensity white light ($1.5 \times 10^{18}$ photons/cm$^{-2}$/s), which was approximately four orders of magnitude higher than what is needed to activate ChR2-expressing retinal cells.[18] We found no retinal thinning, suggestive of no apoptosis in inner retinal cells, and no increase of immune cells (detected by CD45 immunolabeling) at higher light levels, and no increase in GFAP expression as compared to controls. Taken together, these data establish that chronic high-intensity light exposure to the ChR2-treated retina is safe.

The bipolar cell-derived responses shown here are sufficiently robust to drive action potential generation in postsynaptic ganglion cells, despite potential circuit remodeling that may have occurred during later stages of degeneration. Normal ganglion cell responses have a dynamic range of ~2.5 log units,[45,46] whereas our treated *rd10* retinal responses spanned at least 1.4 log units. Response saturation was not observed in these experiments due to limitations in the intensity of the experimental light stimulus. If desired, customizable head wearable glasses could serve to preprocess visual stimuli to provide light amplification, dynamic range compression, local gain control, spatiotemporal processing, and chromatic adjustment to maximize the utility of ChR2 as a therapy for blindness.

## MATERIALS AND METHODS

***Animals.*** WT C57Bl/6J, *rd1* (C57Bl/6J), and *rd10* (C57Bl/6J) were purchased from the Jackson Laboratory (Bar Harbor, ME), and *rd16* (C57Bl/6J) mice were used as previously described.[47] All mice were housed on a 12-hour light-dark cycle in typical room illumination. Mice evaluated in phototoxicity studies (see below) were exposed to a 12-hour light-dark cycle in background light yielding $10^{18}$ photons/cm$^{-2}$/s at 470 nm. All animal procedures were performed according to the Ophthalmic and Vision Research of the Association of Research in Vision and Ophthalmology, and the guidelines approved by the Institutional Animal Care and Use Committees at the University of Florida (Gainesville, FL), the University of Southern California (Los Angeles, CA), the University of California, Berkeley (Berkeley, CA), and Eos Neuroscience, Inc (Los Angeles, CA).

***Plasmid DNA and rAAV production/purification.*** Generation of our transgene construct employed general subcloning techniques. Our therapeutic DNA construct (**Figure 1a**) consisted of a murine-optimized 200 bp enhancer, isolated from the murine metabotropic glutamate receptor subtype 6 gene (*mGRM6*),[20,21] a simian vacuolating virus 40 (SV40) core promoter, and a human codon-optimized ChR2 (hChR2) fused to a heGFP (**Figure 1a**). The mGRM6 200 bp DNA enhancer sequence corresponded to nucleotide positions −8,583 to −8,384 relative to the ATG start codon (kindly provided by Dr Constance Cepko) fused to a Semian virus 40 (SV40) eukaryotic core promoter sequence. The sequence of the enhancer region was 5′–GAT CTC CAG ATG GCT AAA CTT TTA AAT CAT GAA TGA AGT AGA TAT TAC CAA ATT GCT TTT TCA GCA TCC ATT TAG ATA ATC ATG TTT TTT GCC TTT AAT CTG TTA ATG TAG TGA ATT ACA GAA ATA CAT TTC CTA AAT CAT TAC ATC CCC CAA ATC GTT AAT CTG CTA AAG TAC ATC TCT GGC TCA AAC AAG ACT GGT TG–3′. The hChR2-heGFP construct was subcloned into a self-complementary vector, comprised of one WT AAV2 terminal resolution site and one mutant resolution site.

Recombinant AAV vectors were used as a delivery vehicle for the DNA construct. In these experiments, we used a rAAV vector that was generated through site-directed mutagenesis of the Y733F surface-exposed tyrosine residue on the AAV capsid (rAAV8-Y733F) as described previously.[25,48] Vector preparations were produced by the plasmid co-transfection method. The crude iodixanol fraction was further purified and concentrated by column chromatography on a 5 ml HiTrap Q Sepharose column using a Pharmacia AKTA FPLC System (Amersham Biosciences, Piscataway, NJ). The vector was eluted from the column using 215 mmol/1 NaCl, pH 8.0, and the rAAV peak was collected. Vector-containing fractions were then concentrated and buffer exchanged in Alcon BSS with 0.014% Tween 20, using a Biomax 100 K concentrator (Millipore, Billerica, MA). Vector was then tittered for DNase-resistant vector genomes by real-time PCR relative to a standard. Finally, the purity of the vector was determined by silver-stained sodium dodecyl sulfate-polyacrylamide gel electrophoresis, assayed for sterility and lack of endotoxin, and then aliquoted and stored at −80 °C.

***Intraocular administration.*** Mice were anesthetized with intraperitoneal ketamine/xylazine (100 mg/kg ketamine and 16.5 mg/kg xylazine) plus a topical ocular anesthetic (proparacaine 0.5%). Phenylephrine (2.5%) and atropine sulfate (1%) were then dropped into the eye to induce pupil dilation. Once the pupil was fully dilated methylcellulose (2.5%) drops were used to provide a clear view of rodent fundus and to prevent drying of the eye. The anesthetized animal was positioned on its side under a dissecting microscope. The sclera was carefully punctured nasally ~0.5–1 mm anterior to the pars plana with a 30G hypodermic needle. With the bevel of the needle, facing upwards care was taken to avoid the lens. The puncture needle was then removed carefully followed by insertion of blunt needle (33G) through the hole. With just the tip of the blunt needle entered into the anterior chamber, the syringe was turned such that the needle is pointed posterior. By gently sliding the needle in toward the posterior of the eye, the lens is pushed aside slightly to maneuver the needle-tip to the desired injection spot (intravitreal or subretinal). The animals were injected with 1.0 µl of iso-osmotic fluid containing the rAAV vector. Following surgery, veterinary ophthalmic antibacterial ointment was applied to prevent drying of cornea and infection.

***Immunohistochemistry and confocal microscopy.*** Expression of heGFP, GFAP, PKCα arrestin, and CD45 proteins in retina of control and treated animals were evaluated using immunohistochemistry combined with confocal imaging 2 and 10 weeks following subretinal injection of AAV vectors. The eyecup was dissected and immersed in 4% paraformaldehyde in 0.1 mol/l phosphate buffer at pH 7.4. Tissues were sucrose-infiltrated overnight, and they were frozen in optimal cutting temperature compound on dry ice the following day. Ten-micron serial sections of tissues were prepared on a Leica CM 3050 S cryostat (Leica, Mannheim, Germany). The tissue sections were immunolabeled with primary antibodies against rabbit anti-green fluorescent protein (heGFP) IgG (dilution 1:500; Invitrogen, Carlsbad, CA), mouse antiprotein kinase α (PKCα) IgG (dilution 1:100; Santa Cruz Biotechnology, Santa Cruz, CA), mouse anti-GFAP IgG (dilution 1:400; Invitrogen), mouse anti-visual arrestin IgG (dilution 1:250; Santa Cruz Biotechnology) and mouse anti-CD45 (dilution 1:500; eBioscience, San Diego, CA) diluted in the blocking

solution containing 3% bovine serum albumin + 5% normal goat serum. The sections were then incubated with secondary antibodies against rabbit immunoglobulin G (Invitrogen; Alexa Fluor 488, dilution, 1:1000) and mouse immunoglobulin G (Invitrogen; Alexa Fluor 555, dilution, 1:200). Prolong gold antifade mounting media (Invitrogen) containing DAPI was used to mount the sections and to stain cell nuclei. Antibody distribution was visualized using a TCS-SP5 Broadband Spectra laser confocal microscope equipped with a ×20 and ×63 (NA = 1.2) objective (Leica Microsystems, Deerfield, IL). Evaluation of GFP expression in various tissues for biodistribution analysis was performed by epifluorescence microscopy using an AxioVision Zeiss microscope (AxioVision Zeiss, Mannheim, Germany).

***Electrophysiology.*** Multielectrode array recordings were performed on treated *rd10* whole mount retinae, untreated *rd10* negative controls, and WT C57BL/6 positive controls. *Rd10* mice were 290 days old at the time of recording. Six months following subretinal injection of AAV8-Y733F-mGRM6-SV40-hChR2-heGFP, mice were euthanized and eyes were quickly enucleated and placed in physiological saline solution [1.9 g/l sodium bicarbonate (EMD, Gibbstown, NJ), 0.05 g/l kanamycin sulfate (Invitrogen), 8.8 g/l Ames media (Sigma, St Louis, MO)] and equilibrated with 95% $O_2$, 5% $CO_2$ (BIOBLEND; Praxair, Danbury, CT). Eyes were dissected in dim red light by first removing the cornea and vitreous, then the retina was mounted ganglion cell side up onto Millipore filter discs as described.[49] The membrane was carefully cut around the retina and placed ganglion cell side down onto a 60-channel multielectrode array (MEA60 system; Multi Channel Systems, Reutlingen, Germany) for recording as described previously.[13] The 30-µm diameter microelectrodes were spaced 200 µm apart on the array. A custom-made platinum wire and dialysis membrane weight was placed on the retina, which was allowed to settle onto the array for 20 minutes before recording commenced. During recording, a constant perfusion of Ames media (34 °C), equilibrated with 95% $O_2$ and 5% $CO_2$, was provided to the recording chamber at a rate of 6 ml/min. Synaptic transmission was blocked where indicated via bath perfusion of 20 µmol/l l-AP4 (dl-2-amino-4-phosphono-butyric acid), 50 µmol/l CNQX (6-cyano-7-nitroquinoxaline-2,3-dione), and 50 µmol/l CPP [(±)-3-(2-carboxypiperazin-4-yl)propyl-1-phosphonic acid]. All chemicals were purchased from Tocris (Ellisville, MO). No all-*trans*-retinal was provided during recording. Signals were recorded using MC Rack (Multi Channel Systems) and filtered between 500 Hz (low cutoff) and 3500 Hz (high cutoff). Spikes were extracted and sorted using an algorithm based on the first three PCA components of 1 ms shape of the spike using Offline Sorter V.3 (Plexon, Dallas, TX), and plotted using Matlab (Mathworks, Natick, MA).

***Behavioral evaluation.*** We used a six alternative, forced-choice water maze task to measure visual performance in mice navigating a water maze task. The water maze apparatus (**Figure 4a**) consisted of six tunnels, and the target denoted a raised platform at the end of a tunnel. The target was marked with a 4 × 6 LED array (LEDs with broad spectral composition) directly above the platform. After each trial, the target was moved randomly to another tunnel and the platform rinsed. Times to find the target varied from 2 to 45 seconds. During the training period, if a mouse took 45 seconds or more to find the target, it was guided to the platform using a wand. Testing was performed under controlled uniform illumination and the photon flux (for the peak sensitivity of ChR2, ~470 nm) was measured using a photometer before each training or threshold measurement session.

During the training period the photon flux of the stimulus at 470 nm, as measured from the center of the maze (*i.e.*, where the each mouse begins their trial), was ~$3.5 \times 10^{18}$ photons/cm$^2$/s. During each session, each mouse performed four or five trials and the time to escape was measured. For sham-injected and -treated mice, we conducted a total of 14 training sessions; for WT, we conducted 7 training sessions, which was enough for the time to find the target to asymptote (**Figure 4**).

Next, we measured the visual threshold for this water maze task. To do this, we measured behavioral performance at light levels starting at ~$3.5 \times 10^{12}$ photons/cm$^{-2}$/s, and with increasing light levels by an order of magnitude, to $3.5 \times 10^{18}$ photons/cm$^{-2}$/s, for a total set of measurements at each light level. A total of 15 trials for each mouse were collected at each light level.

***Biodistribution analysis.*** The spread of vector DNA and GFP expression in distant tissues was determined by immunohistochemistry and qPCR in samples collected at termination. Tissue samples from heart, liver, spleen, lung, kidney, muscle, inguinal lymph node, ovary, skin, jejunum, brain, and eye were collected. Precautions were taken to avoid cross-contamination while harvesting tissues. Once removed, each tissue was held over a Petri dish and rinsed with sterile phosphate-buffered saline. The tissue was placed in a weighing boat and weighted. Samples for immunohistochemistry were fixed in 4% paraformaldehyde in 0.1 mol/l phosphate buffer, immersed in 30% sucrose overnight and frozen the next day in optimal cutting temperature. PCR samples were collected into Eppendorf tubes containing 500 µl RNA later (Qiagen, Hilden, Germany) and were stored at 4 °C until used. For qPCR analysis, tissues were digested, and the DNA was isolated, using Bio-Rad Instagene Matrix, and DNA was quantified using a Bio-Rad qPCR. Expression of ChR2 and β-actin was analyzed from 50 ng of DNA by quantitative real-time-PCR and expressed as a ratio of ChR2 copy numbers to β-actin copy numbers (two per cell). Primers were designed to amplify a sequence of the ChR2 DNA: 5′-CAATGTTACTGTGCCGGATG-3′ (forward) and 5′-ATTTCAATCGCGCACACATA-3′ (reverse) and β-actin expression was analyzed using the primers: 5′-CCAGGCATTGCTGACAGGAT-3′ (forward) and 5′-CCCACCCTCACCAAGCTAAG-3′ (reverse). Fifty nanograms of DNA from each tissue, including the treated eye, were analyzed in triplicate, and the double-stranded ChR2 was tagged and quantified using SYBR green. Forty cycles were run with standard curves from plasmid DNA-containing ChR2 and DNA with β-actin. Any value <0.05 copies of ChR2 per copy of β-actin was defined as the threshold and not reported.

***Hematology and serum chemistry.*** Before blood collection, individual body weights were recorded. Five hundred microliters of blood were collected from the heart using a 23-gauge needle on a 1-ml syringe. The needle was removed and the blood samples were placed into separate tubes for comprehensive complete blood count and serum chemistry analyses. Samples were sent to IDEXX Laboratories (West Sacramento, CA) for analysis. Hematology parameters included RBC count, hemoglobulin, hematocrit, erythrocyte indexes (mean corpuscular volume, MCH, and MCHC), white blood cell differential, platelet count, smear evaluation for RBC and white blood cell blood morphology and parasite screen, pathologist review of abnormal cells, reticulocyte count and absolute reticulocyte count. Serum chemistries included albumin, albumin/globulin ratio, alkaline phosphatase, alanine aminotransferase (SGPT), aspartate aminotransferase (SGOT), bicarbonate, direct bilirubin, indirect bilirubin, total bilirubin, BUN, BUN/creatinine ratio, calcium, chloride, cholesterol, creatine kinase, creatinine, globulin, glucose, phosphorus, potassium, sodium, sodium/potassium ratio, and total protein.

## SUPPLEMENTARY MATERIAL

**Figure S1.** Behavioral training.

**Figure S2.** H&E and IHC staining examining transgene expression (hChR2-heGFP) in (**a**,**b**,**c**) retinae, (**d**,**e**,**f**) brain, and (**g**,**h**,**i**) heart of the *rd10* mouse.

**Table S1.** Safety studies.

**Table S2.** Serum chemistry analysis from *rd10* mice 10 weeks postinjection with BSS, low-dose and high-dose AAV vectors.

## ACKNOWLEDGMENTS

We thank Constance Cepko (Harvard University) for kindly providing the use of her regulatory sequence. This research was funded by NIH grants EY019201, EY13729, EY11123, and EY08571; The Wallace H. Coulter Foundation; The Baxter Foundation; The Macular Vision Research Foundation; Foundation Fighting Blindness; Hope for Vision; Research to Prevent Blindness. M.M.D. is an employee of Eos Neuroscience, Inc. and holds equity; K.P.G. is consultant to Eos Neuroscience, Inc. and holds equity; J.L., none; K.A.S., none; E.S.B. is a cofounder of Eos Neuroscience, Inc. and holds equity; J.A.L. is a consultant to Eos Neuroscience, Inc.; A.C.A. is a consultant for Eos Neuroscience, Inc. and holds equity; R.J., none; S.E.B., none; S.L.B., none; G.M.G., none; B.C.M. is an employee and cofounder of Eos Neuroscience, Inc. and holds equity; A.P.S. is on the scientific advisory board of Eos Neuroscience, Inc. and holds equity; W.W.H. is on the scientific advisory board of Eos Neuroscience, Inc. and holds equity in AGTC, Inc. that may, in the future, commercialize some aspects of this work; A.H. is an employee and cofounder of Eos Neuroscience, Inc. and holds equity.

## REFERENCES

1. Chader, GJ (2002). Animal models in research on retinal degenerations: past progress and future hope. *Vision Res* **42**: 393–399.
2. Congdon, N, O'Colmain, B, Klaver, CC, Klein, R, Muñoz, B, Friedman, DS *et al.*; Eye Diseases Prevalence Research Group. (2004). Causes and prevalence of visual impairment among adults in the United States. *Arch Ophthalmol* **122**: 477–485.
3. Bainbridge, JW, Smith, AJ, Barker, SS, Robbie, S, Henderson, R, Balaggan, K *et al.* (2008). Effect of gene therapy on visual function in Leber's congenital amaurosis. *N Engl J Med* **358**: 2231–2239.
4. Hauswirth, WW, Aleman, TS, Kaushal, S, Cideciyan, AV, Schwartz, SB, Wang, L *et al.* (2008). Phase I trial of Leber congenital amaurosis due to RPE65 mutations by ocular subretinal injection of adeno-associated virus gene vector: Short-term results. *Hum Gene Ther* **19**: 979–990.
5. Daiger, SP, Bowne, SJ and Sullivan, LS (2007). Perspective on genes and mutations causing retinitis pigmentosa. *Arch Ophthalmol* **125**: 151–158.
6. Jones, BW, Watt, CB, Frederick, JM, Baehr, W, Chen, CK, Levine, EM *et al.* (2003). Retinal remodeling triggered by photoreceptor degenerations. *J Comp Neurol* **464**: 1–16.
7. de Balthasar, C, Patel, S, Roy, A, Freda, R, Greenwald, S, Horsager, A *et al.* (2008). Factors affecting perceptual thresholds in epiretinal prostheses. *Invest Ophthalmol Vis Sci* **49**: 2303–2314.
8. Horsager, A, Greenwald, SH, Weiland, JD, Humayun, MS, Greenberg, RJ, McMahon, MJ *et al.* (2009). Predicting visual sensitivity in retinal prosthesis patients. *Invest Ophthalmol Vis Sci* **50**: 1483–1491.
9. Zrenner, E, Bartz-Schmidt, KU, Benav, H, Besch, D, Bruckmann, A, Gabel, VP *et al.* (2010). Subretinal electronic chips allow blind patients to read letters and combine them to words. *Proc Biol Sci* (epub ahead of print).
10. Horsager, A, Boynton, GM, Greenberg, RJ, and Fine, I (2011). Temporal interactions during paired-electrode stimulation in two retinal prosthesis subjects. *Invest Ophthalmol Vis Sci* **52**: 549–557.
11. Horsager, A, Greenberg, RJ and Fine, I (2010). Spatiotemporal interactions in retinal prosthesis subjects. *Invest Ophthalmol Vis Sci* **51**: 1223–1233.
12. Roska, B and Werblin, F (2001). Vertical interactions across ten parallel, stacked representations in the mammalian retina. *Nature* **410**: 583–587.
13. Roska, B, Molnar, A and Werblin, FS (2006). Parallel processing in retinal ganglion cells: how integration of space-time patterns of excitation and inhibition form the spiking output. *J Neurophysiol* **95**: 3810–3822.
14. Nagel, G, Ollig, D, Fuhrmann, M, Kateriya, S, Musti, AM, Bamberg, E *et al.* (2002). Channelrhodopsin-1: a light-gated proton channel in green algae. *Science* **296**: 2395–2398.
15. Boyden, ES, Zhang, F, Bamberg, E, Nagel, G and Deisseroth, K (2005). Millisecond-timescale, genetically targeted optical control of neural activity. *Nat Neurosci* **8**: 1263–1268.
16. Bi, A, Cui, J, Ma, YP, Olshevskaya, E, Pu, M, Dizhoor, AM *et al.* (2006). Ectopic expression of a microbial-type rhodopsin restores visual responses in mice with photoreceptor degeneration. *Neuron* **50**: 23–33.
17. Lin, B, Koizumi, A, Tanaka, N, Panda, S and Masland, RH (2008). Restoration of visual function in retinal degeneration mice by ectopic expression of melanopsin. *Proc Natl Acad Sci USA* **105**: 16009–16014.
18. Thyagarajan, S, van Wyk, M, Lehmann, K, Löwel, S, Feng, G and Wässle, H (2010). Visual function in mice with photoreceptor degeneration and transgenic expression of channelrhodopsin 2 in ganglion cells. *J Neurosci* **30**: 8745–8758.
19. Greenberg, KP, Pham, A and Werblin, FS (2011). Differential targeting of optical neuromodulators to ganglion cell soma and dendrites allows dynamic control of center-surround antagonism. *Neuron* **69**: 713–720.
20. Kim, DS, Matsuda, T and Cepko, CL (2008). A core paired-type and POU homeodomain-containing transcription factor program drives retinal bipolar cell gene expression. *J Neurosci* **28**: 7748–7764.
21. Lagali, PS, Balya, D, Awatramani, GB, Münch, TA, Kim, DS, Busskamp, V *et al.* (2008). Light-activated channels targeted to ON bipolar cells restore visual function in retinal degeneration. *Nat Neurosci* **11**: 667–675.
22. Muramatsu, T, Nakamura, A and Park, HM (1998). *In vivo* electroporation: a powerful and convenient means of nonviral gene transfer to tissues of living animals (Review). *Int J Mol Med* **1**: 55–62.
23. Dinculescu, A, Glushakova, L, Min, SH and Hauswirth, WW (2005). Adeno-associated virus-vectored gene therapy for retinal disease. *Hum Gene Ther* **16**: 649–663.
24. Douar, AM, Poulard, K, Stockholm, D and Danos, O (2001). Intracellular trafficking of adeno-associated virus vectors: routing to the late endosomal compartment and proteasome degradation. *J Virol* **75**: 1824–1833.
25. Petrs-Silva, H, Dinculescu, A, Li, Q, Min, SH, Chiodo, V, Pang, JJ *et al.* (2009). High-efficiency transduction of the mouse retina by tyrosine-mutant AAV serotype vectors. *Mol Ther* **17**: 463–471.
26. Mazzoni, F, Novelli, E and Strettoi, E (2008). Retinal ganglion cells survive and maintain normal dendritic morphology in a mouse model of inherited photoreceptor degeneration. *J Neurosci* **28**: 14282–14292.
27. Hood DC and Finkelstein, MAF (1986). *Sensitivity to Light*. Wiley: New York.
28. Bourin, M and Hascoët, M (2003). The mouse light/dark box test. *Eur J Pharmacol* **463**: 55–65.
29. Thomas, BB, Seiler, MJ, Sadda, SR, Coffey, PJ and Aramant, RB (2004). Optokinetic test to evaluate visual acuity of each eye independently. *J Neurosci Methods* **138**: 7–13.
30. Hayes, JM and Balkema, GW (1993). Elevated dark-adapted thresholds in hypopigmented mice measured with a water maze screening apparatus. *Behav Genet* **23**: 395–403.
31. Sampath, AP, Strissel, KJ, Elias, R, Arshavsky, VY, McGinnis, JF, Chen, J *et al.* (2005). Recoverin improves rod-mediated vision by enhancing signal transmission in the mouse retina. *Neuron* **46**: 413–420.
32. Han, X, Qian, X, Bernstein, JG, Zhou, HH, Franzesi, GT, Stern, P *et al.* (2009). Millisecond-timescale optical control of neural dynamics in the nonhuman primate brain. *Neuron* **62**: 191–198.
33. Ekström, P, Sanyal, S, Narfström, K, Chader, GJ and van Veen, T (1988). Accumulation of glial fibrillary acidic protein in Müller radial glia during retinal degeneration. *Invest Ophthalmol Vis Sci* **29**: 1363–1371.
34. Streilein, JW, Takeuchi, M and Taylor, AW (1997). Immune privilege, T-cell tolerance, and tissue-restricted autoimmunity. *Hum Immunol* **52**: 138–143.
35. Nishida, T and Taylor, AW (1999). Specific aqueous humor factors induce activation of regulatory T cells. *Invest Ophthalmol Vis Sci* **40**: 2268–2274.
36. Marc, RE, Jones, BW, Anderson, JR, Kinard, K, Marshak, DW, Wilson, JH *et al.* (2007). Neural reprogramming in retinal degeneration. *Invest Ophthalmol Vis Sci* **48**: 3364–3371.
37. Punzo, C and Cepko, C (2007). Cellular responses to photoreceptor death in the rd1 mouse model of retinal degeneration. *Invest Ophthalmol Vis Sci* **48**: 849–857.
38. Ivanova, E and Pan, ZH (2009). Evaluation of the adeno-associated virus mediated long-term expression of channelrhodopsin-2 in the mouse retina. *Mol Vis* **15**: 1680–1689.
39. Fields, RD, Lee, PR and Cohen, JE (2005). Temporal integration of intracellular Ca2+ signaling networks in regulating gene expression by action potentials. *Cell Calcium* **37**: 433–442.
40. Gamlin, PD, McDougal, DH, Pokorny, J, Smith, VC, Yau, KW and Dacey, DM (2007). Human and macaque pupil responses driven by melanopsin-containing retinal ganglion cells. *Vision Res* **47**: 946–954.
41. Ecker, JL, Dumitrescu, ON, Wong, KY, Alam, NM, Chen, SK, LeGates, T *et al.* (2010). Melanopsin-expressing retinal ganglion-cell photoreceptors: cellular diversity and role in pattern vision. *Neuron* **67**: 49–60.
42. Dacey, DM, Liao, HW, Peterson, BB, Robinson, FR, Smith, VC, Pokorny, J *et al.* (2005). Melanopsin-expressing ganglion cells in primate retina signal colour and irradiance and project to the LGN. *Nature* **433**: 749–754.
43. Wässle, H, Puller, C, Müller, F and Haverkamp, S (2009). Cone contacts, mosaics, and territories of bipolar cells in the mouse retina. *J Neurosci* **29**: 106–117.
44. Remé, CE, Grimm, C, Hafezi, F, Marti, A and Wenzel, A (1998). Apoptotic cell death in retinal degenerations. *Prog Retin Eye Res* **17**: 443–464.
45. Barlow, HB and Levick, WR (1969). Changes in the maintained discharge with adaptation level in the cat retina. *J Physiol (Lond)* **202**: 699–718.
46. Thibos, LN and Werblin, FS (1978). The response properties of the steady antagonistic surround in the mudpuppy retina. *J Physiol (Lond)* **278**: 79–99.
47. Cideciyan, AV, Rachel, RA, Aleman, TS, Swider, M, Schwartz, SB, Sumaroka, A *et al.* (2011). Cone photoreceptors are the main targets for gene therapy of NPHP5 (IQCB1) or NPHP6 (CEP290) blindness: generation of an all-cone Nphp6 hypomorph mouse that mimics the human retinal ciliopathy. *Hum Mol Genet* **20**: 1411–1423.
48. Zhong, L, Li, B, Mah, CS, Govindasamy, L, Agbandje-McKenna, M, Cooper, M *et al.* (2008). Next generation of adeno-associated virus 2 vectors: point mutations in tyrosines lead to high-efficiency transduction at lower doses. *Proc Natl Acad Sci USA* **105**: 7827–7832.
49. Koizumi, A, Zeck, G, Ben, Y, Masland, RH and Jakobs, TC (2007). Organotypic culture of physiologically functional adult mammalian retinas. *PLoS ONE* **2**: e221.

# SUPPLEMENTARY INFORMATION

**FROM:**

## Virally delivered Channelrhodopsin-2 Safely and Effectively Restores Visual Function in Multiple Mouse Models of Blindness

M Mehdi Doroudchi, Kenneth P Greenberg, Jianwen Liu, Kimberly A Silka, Edward S Boyden, Jennifer A Lockridge, A Cyrus Arman, Ramesh Janani, Shannon E Boye, Sanford L Boye, Gabriel M Gordon, Benjamin C Matteo, Alapakkam P Sampath, William W Hauswirth and Alan Horsager

**Download plugins**

### Figure S1. (tiff 122K)

Behavioral training. We trained the sham injected (injected with saline solution) and ChR2-treated mice for 14 days (x-axis). As the wild-type learned the task much more quickly, only 7 days of training were necessary. Time to find the platform (in seconds) is on the y-axis.

### Figure S2. (tiff 1,605K)

H&E and IHC staining examining transgene expression (hChR2-heGFP) in (**a**,**b**,**c**) retinae, (**d**,**e**,**f**) brain, and (**g**,**h**,**i**) heart of the *rd10* mouse. Tissues shown here were collected 10 weeks post-injection and examined for eGFP fluorescence (B, E, H). Negative controls were made to account from any non-specific binding of the secondary (fluorescent) antibody (C, F, I). One week data (not shown) did not show any heGFP expression in any organ other than the eye.

### Table S1. (doc 34K)

Safety studies. There were 5 different safety studies: biodistribution, ocular toxicology, hematology, delayed-type hypersensitivity (DTH), and phototoxicity. Please note that, in the ocular toxicology, two doses were evaluated (i.e., high and low).

### Table S2. (doc 68K)

Serum chemistry analysis from *rd10* mice 10 weeks postinjection with BSS, low-dose and high-dose AAV vectors.

**Download plugins**

***Molecular Therapy*** ISSN 1525-0016 EISSN 1525-0024

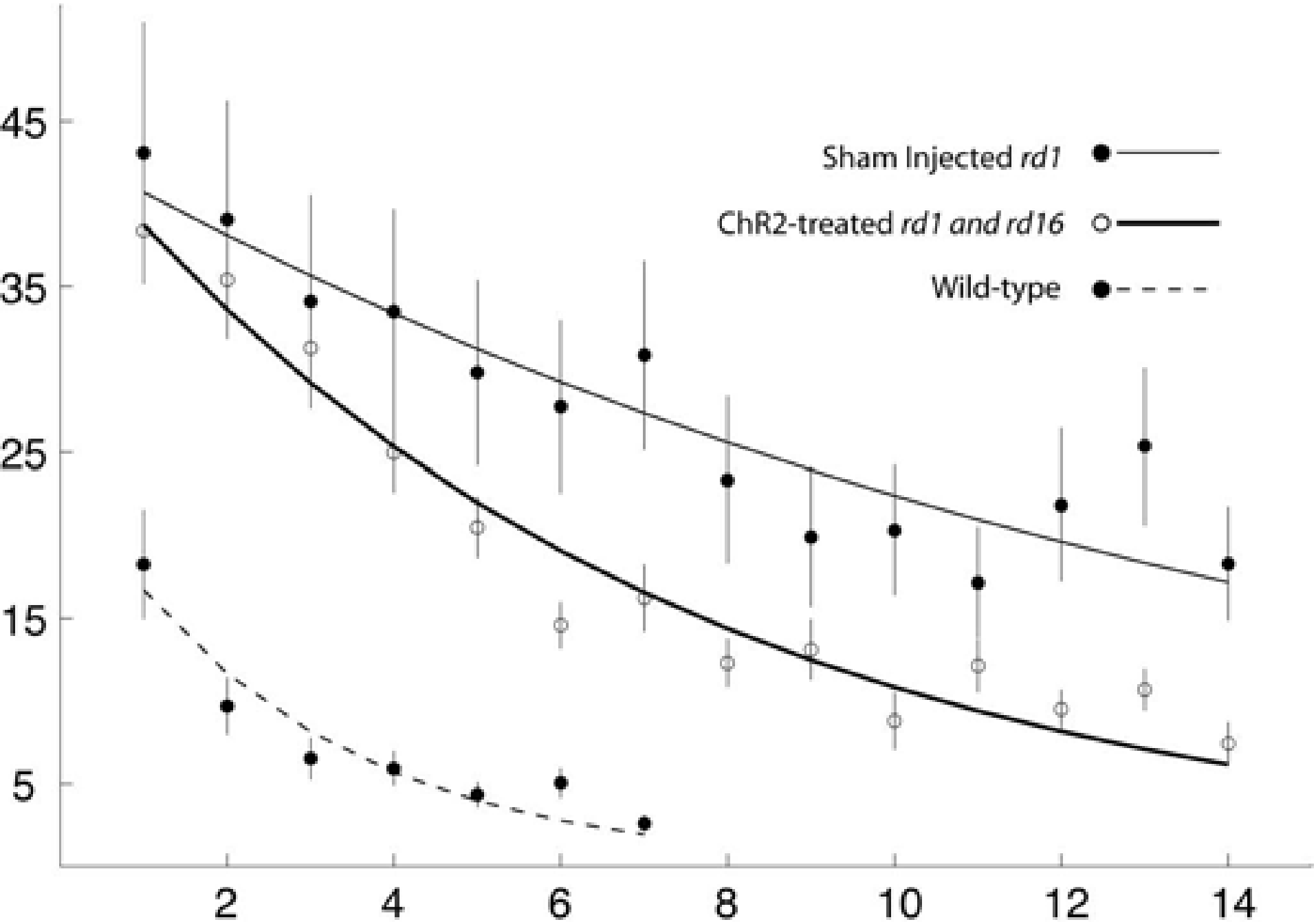
45
35
25
15
5
2
4
6
8
10
12
14
Sham Injected rd1
ChR2-treated rd1 and rd16
Wild-type

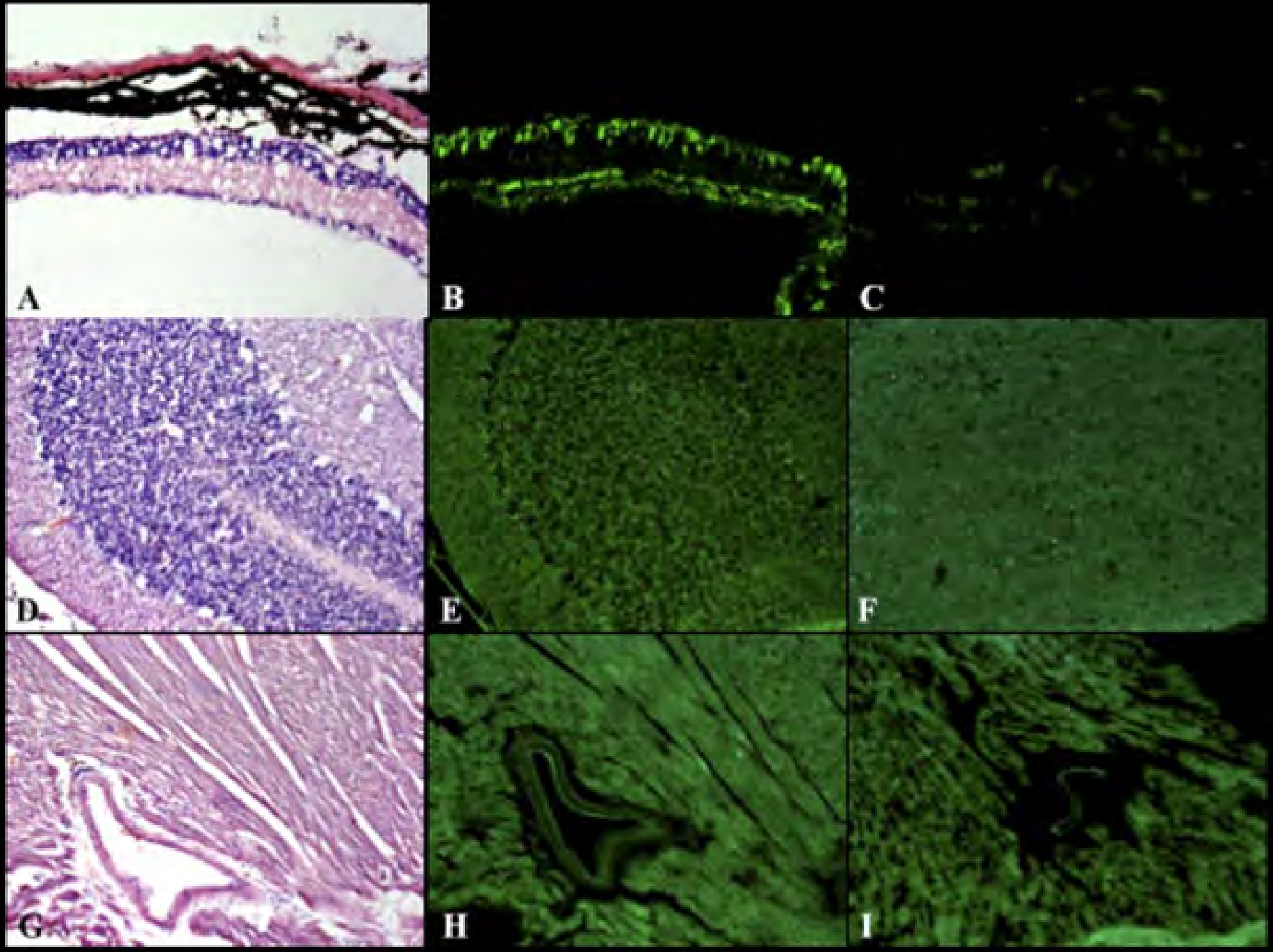
A
B
C
D
E
F
G
H
I

| Group | Study | Number (M/F) | Vector | Titer (dose) | Necropsy |
|---|---|---|---|---|---|
| 1A | Biodistribution (IHC, qPCR) | 2F | BSS | n/a | 1 Week |
| 1B | | 2F | BSS | n/a | 10 Weeks |
| 2A | | 4F | AAV8-Y733F | $2.88 \times 10^{12}$ | 1 Week |
| 2B | | 4F | $2.88 \times 10^{12}$ | $2.88 \times 10^{12}$ | 10 Weeks |
| 3A | Ocular Toxicology, Hematology | 2M, 2F | BSS | n/a | 2 Weeks |
| 3B | | 2M, 2F | BSS | n/a | 10 Weeks |
| 4A | | 2M, 2F | AAV8-Y733F | $2.88 \times 10^{10\ (low)}$ | 2 Weeks |
| 4B | | 2M, 2F | AAV8-Y733F | $2.88 \times 10^{10\ (low)}$ | 10 Weeks |
| 5A | | 2M, 2F | AAV8-Y733F | $2.88 \times 10^{12\ (high)}$ | 2 Weeks |
| 5B | | 2M, 2F | AAV8-Y733F | $2.88 \times 10^{12\ (high)}$ | 10 Weeks |
| 6 | Delayed-Type Hypersensitivity | 2M, 2F | AAV8-Y733F | $2.88 \times 10^{12}$ | n/a |
| 7A | Phototoxicity | 1M, 1F | BSS | n/a | 2 Weeks |
| 7B | | 1M, 1F | BSS | n/a | 10 Weeks |
| 8A | | 2M, 2F | AAV8-Y733F | $2.88 \times 10^{12}$ | 2 Weeks |
| 8B | | 2M, 2F | AAV8-Y733F | $2.88 \times 10^{12}$ | 10 Weeks |

| Serum Parameter | Unit of Measure | Normal Range | Control # 1 (F) | Control # 1 (M) | Control # 2 (M) | Low Dose # 1 (M) | Low Dose # 2 (M) | Low Dose # 1 (F) | Low Dose # 2 (F) | High Dose # 1 (F) | High Dose # 2 (F) | High Dose # 1 (M) |
|---|---|---|---|---|---|---|---|---|---|---|---|---|
| Alk. Phosph. | IU/L | 47-85 | 92 | 58 | 42 | 57 | 42 | 92 | 93 | 81 | 91 | 60 |
| SGPT (ALT) | IU/L | - | 45 | 27 | 38 | 96 | 22 | 46 | 49 | 24 | 25 | 18 |
| SGOT (AST) | IU/L | - | 143 | 188 | 101 | 117 | 57 | 168 | 95 | 69 | 77 | 56 |
| CPK | IU/L | - | 964 | 473 | 616 | 156 | 196 | 450 | 276 | 343 | 281 | 407 |
| Albumin | g/dL | 3.3-3.5 | 2.9 | 2.5 | 2.5 | 2.7 | 2.8 | 2.8 | 3 | 2.7 | 2.8 | 2.8 |
| Total Protein | g/dL | 6.0-6.4 | 4.8 | 4.4 | 4.5 | 5 | 5 | 4.8 | 4.9 | 4.7 | 5.1 | 5 |
| Globulin | g/dL | - | 1.9 | 1.9 | 2 | 2.3 | 2.2 | 2 | 1.9 | 2 | 2.3 | 2.2 |
| Total Bilirubin | mg/dL | 0.0-0.9 | 0.3 | 0.1 | 0.1 | 0.2 | 0.1 | 0.2 | 0.2 | 0.2 | 0.3 | 0.1 |
| Direct Bilirubin | mg/dL | - | 0 | 0 | 0.1 | 0.1 | 0 | 0.1 | 0.1 | 0.1 | 0.1 | 0 |
| BUN | mg/dL | - | 38 | 33 | 33 | 30 | 35 | 35 | 34 | 33 | 34 | 31 |
| Creatinine | mg/dL | 0.5-1.4 | 0.3 | 0.2 | 0.2 | 0.2 | 0.2 | 0.2 | 0.2 | 0.2 | 0.2 | 0.2 |
| Cholestrol | mg/dL | 29-110 | 74 | 89 | 91 | 104 | 112 | 69 | 75 | 88 | 87 | 116 |
| Glucose | mg/dL | 47-137 | 304 | 324 | 303 | 220 | 245 | 217 | 257 | 250 | 243 | 332 |
| Calcium | mg/dL | 4.8-7.4 | 9.2 | 9 | 8.4 | 8.2 | 8.6 | 8.6 | 8.7 | 8.9 | 8.4 | 8.5 |
| Phosphorus | mg/dL | 5.3-7.9 | 10.3 | 9.3 | 7.2 | 6.3 | 5.1 | 6.7 | 6.2 | 7.7 | 6.4 | 5.7 |
| Bicarbonate | meq/L | - | 8 | 18 | 18 | 13 | 16 | 14 | 14 | 10 | 16 | 20 |
| Chloride | meq/L | 96-129 | 114 | 112 | 113 | 113 | 115 | 116 | 115 | 117 | 112 | 111 |
| Potassium | meq/L | 5.3-5.6 | 6.5 | 5 | 4.1 | 5.7 | 4.1 | 4.6 | 4.4 | 4.2 | 6.5 | 5.2 |
| Sodium | meq/L | 135-141 | 147 | 147 | 148 | 150 | 151 | 146 | 149 | 152 | 141 | 146 |
| A/G Ratio | | - | 1.5 | 1.3 | 1.3 | 1.2 | 1.3 | 1.4 | 1.6 | 1.4 | 1.2 | 1.3 |
| B/C Ratio | | - | 126 | 165 | 165 | 150 | 175 | 175 | 170 | 165 | 170 | 155 |
| Indirect Bilirubin | mg/dL | - | 0.3 | 0.1 | 0 | 0.1 | 0.1 | 0.1 | 0.1 | 0.1 | 0.2 | 0.1 |
| Na/K Ratio | | - | 23 | 29 | 36 | 26 | 37 | 32 | 34 | 36 | 22 | 28 |